Detection and Prevention of Hot Spots by Monitoring the Dynamic Conductance of PV Cells 2018-04-30

William P. Lamb[1], Dallon E. Asnes[1], Jonathan Kupfer[2], Florence J. Walsh[2], Richard C. Haskell[3], Peter N. Saeta[3], and Qimin Yang[2]

[1] Physics Department, Pomona College, Claremont, California 91711, USA

[2] Engineering and [3] Physics Departments, Harvey Mudd College, Claremont, California 91711, USA

ABSTRACT: Hot spotting on photovoltaic (PV) cells is a considerable concern for the solar industry in terms of physical damage, power loss, lifetime reliability, and manufacturing costs. The current mitigation technique of employing bypass diodes only partially reduces the effects of hot spots, limiting the power dissipation across a shaded cell to the accumulated power from a string of cells instead of from an entire panel. Alternative methods exist that actively control the operating current and/or voltage of a string of cells so that a partially shaded cell is not forced into reverse bias. We explore the behavior of individual PV cells when externally forced into reverse bias. Results show that cells in reverse bias can suffer significant heating and structural damage, with desoldering of cell-tabbing and discolorations on the front cell surface. We also explore a proposed solution to reverse bias patented by Kernahan et al. [1] that detects and prevents hot spots caused by reverse bias.

I. INTRODUCTION

Considerable literature exists that explores the behavior of solar cells connected in series to form a string, with a growing community recognizing the dangers of reverse bias [2–12]. Although much research on reverse bias and hot spots has been conducted, Kernahan et al. [1] is one of the first to offer a technique for regulating and preventing reverse bias completely [8, 12–15]. Other sources have offered methods for detecting reverse bias but have fallen short of procedures for controlling it [7, 9–11].

Solar cells convert light into electrical current by harnessing the energy of incident photons to drive electrons across the built-in electric field of the cell's *p-n* junction. This electrical current flows through a circuit to power a resistive load attached across the *p*-type and *n*-type terminals of the cell (see Figure 1(a)). Cells that are partially shaded, or those that receive lower intensity light, output less current than cells operating under normal conditions. However, circuit elements in series must have the same current flowing through each of them. When a cell receives less light than the other cells in its series string, that cell outputs less current than the rest. When driven by fully illuminated cells, at a higher current output than can be achieved when shaded, partially-shaded solar cells may suffer from hot spots due to power dissipation.

These hot spots show not only that the panel is losing electrical power output in the form of heat, but also that permanent structural damage may be possible, especially across repeated hot-spotting events. One major cause of hot spots and this power dissipation is that partially-shaded cells are forced into reverse bias to maintain current production to match the output of fully-illuminated cells in a string. When in reverse bias, a cell dissipates power instead of generating it, and in extreme cases converts the entire power production of a substring of illuminated cells into heat in a single, partially-shaded cell. Any solution that seeks to prevent hot spots must take this reverse bias into account.

II. OPERATION & CONTROL OF A PV CELL

A. IV curve and Operating Point

The current produced by an illuminated photovoltaic cell depends both on the level of illumination and on the voltage across it. More light means that more electrons

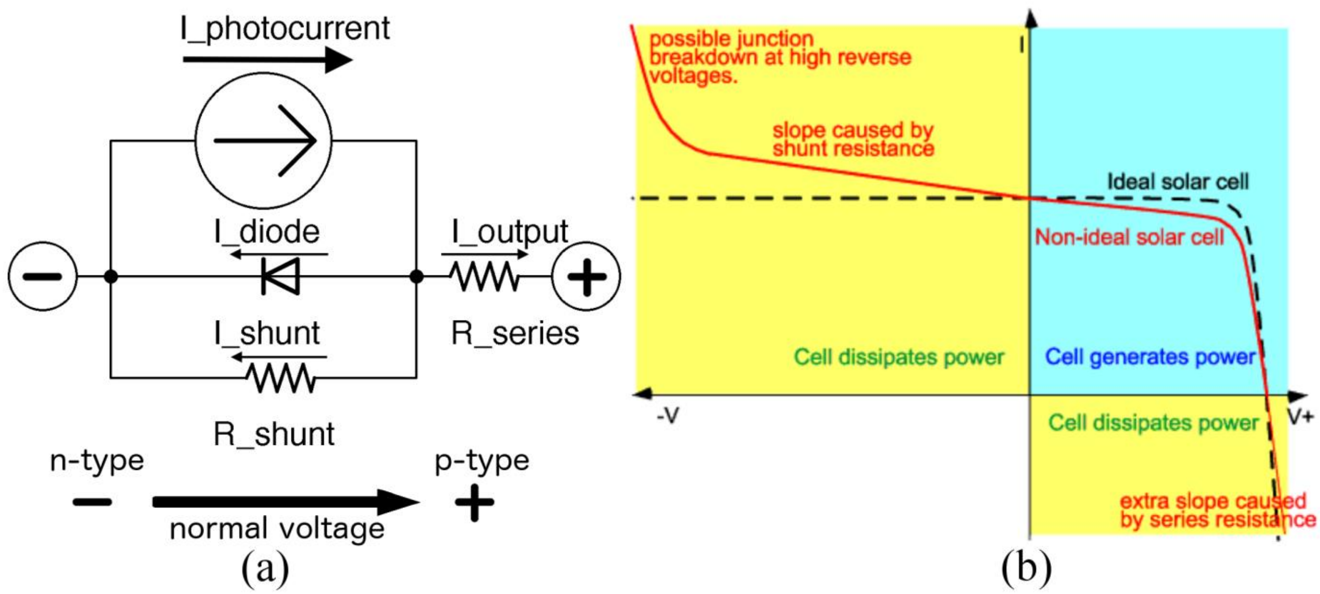

FIG. 1. Solar cell single diode model: (a) circuit diagram in forward bias (b) expanded IV curve (Figure from[5]) Note that the circuit diagram in (a) is only a model of the behavior of the cell, and masks the underlying physics of the *p-n* junction. The slope caused by shunt resistance as seen in (b) is caused by a slight increase in the size of the depletion region in the junction.

are excited and contribute to current, so illumination and current are directly proportional. The voltage determines the operating point along the IV curve. As the voltage increases to its open-circuit point, the current generation decreases to zero. As the voltage difference across the terminals of the cell decreases to zero, the cell approaches short-circuit current (see Figure 1 (b)).

Under normal operating conditions, the cell is forward-biased, meaning that the flow of current through the cell is also the direction of increasing voltage, or that there is a positive voltage difference going from the *n*-type to the *p*-type terminals: $V_p - V_n > 0$. However, due to outside influences (such as other cells in the string) the voltage difference across the cell can drop to zero or even become negative. In the latter case, this negative voltage differential across the cell is termed reverse-bias, and the *n*-type contact of the cell is at a higher voltage than the *p*-type contact: $V_p - V_n < 0$. For a real cell under illumination, the current output increases slightly as the voltage decreases [16]. This phenomenon is accounted for in the circuit model in Fig. 1 (a) in the form of the shunt resistor. The diode in the circuit model helps account for the voltage gain across the cell, and "turns off" as the voltage decreases towards reverse bias. The main part of the cell diagram is the current generator at the top, which converts incident photons to current. The series resistor accounts for a small power loss in the cell itself (the cell material is not a superconductor). However, in reverse bias the shunt resistance accounts for the large power dissipation in the cell, increasing the total current output above that of the photocurrent at the cost of a large voltage drop across the shunt resistor and thereby the cell itself.

B. Conductance as a Detection Parameter

Photovoltaic cells under forward bias (i.e., normal operating conditions) do not undergo hot spots, or at least do not undergo significant heating, extreme enough to damage the cell or affect its lifetime [13]. Only when industry-grade cells go into reverse bias do concerns about hot spotting become appreciable. Hot spots are a significant source of concern for the solar industry, and can cause cells or panels to degrade or fail, and may even start fires [3–5, 17, 18].

When analyzing solar cells connected in series to form strings, conductance is the physically relevant parameter on which to focus. The conductance of a cell is the inverse of its resistance. The dynamic conductance is defined to be the slope of the cell's nonlinear IV curve at a particular (I,V) operating point:

$$G_{dynamic} = \frac{dI}{dV} \tag{1}$$

These changes in current and voltage are usually the result of small externally applied changes in operating voltage and are observed over a short period of time. Dynamic conductance in series adds like resistance in parallel: the total dynamic conductance of a string of cells is always lower than the lowest individual dynamic conductance (Eqn. 2). The dynamic conductance of a cell goes toward zero as the cell approaches reverse bias, so the dynamic conductance of a partially-shaded cell dominates the total dynamic conductance of the string.

$$\frac{1}{G_{total}} = \frac{1}{G_1} + \frac{1}{G_2} + \frac{1}{G_3} + \cdots \tag{2}$$

As any cell approaches reverse bias, its dynamic conductance falls to zero. By monitoring the dynamic conductance of a series of cells, reverse bias in any cell of the series can be detected. Once recognized, it is possible to prevent the cell from going into reverse bias by adjusting the IV operating point of the string of cells.

III. EXPERIMENTAL DESIGN AND METHODS

Testing was performed on a single, grade A Everbright solar cell (6" x 6") to first characterize an IV curve and then force a reverse bias voltage. These reverse bias conditions simulated the performance of a partially-shaded cell connected in series with a string of fully-illuminated cells. An HP6267B power supply was used to externally force a voltage across the terminals of the solar cell. Two SBR20A200CT 200V 20A diodes were placed in series between the power supply and the cell terminals to create an offset voltage, allowing the cell to be operated from open circuit through reverse bias. By using a power supply across the terminals of a cell, an external voltage can be applied that defines the operating point of the cell on its IV curve. The charge controller on a standard panel exhibits this exact controlling behavior; by adjusting the voltage it applies across a string of cells, it can control the resultant current output. There are also other implementations that control the current drawn from the cells instead of the voltage across the string [13].

An ETC 750 Spotlight connected to a variac power source was used to provide illumination and calibrate the cell. The variac allowed control of the irradiance to match one-sun conditions. During calibration, the spotlight power was adjusted to produce the cell's rated short-circuit current at zero volts. In this step the cell receives the intensity of light in its absorption spectrum that it would expect at one sun, and the rest of the light generated by the spotlight is converted to heat. The temperature of the cell at short circuit during this setup is used to calibrate the temperature changes experienced in the rest of the experiment.

To measure the current and voltage outputs of the cell during the IV curve sweep, two Tektronix DM2510G multimeters were used, one in auto-scale volts mode, and the other in fixed-scale 10A mode. A Fluke infrared camera (IR Flexcam TI45) was used to take pictures of the cell at each data point, measuring the temperature of the cell during the voltage sweep and into reverse bias.

The voltmeter directly measured the voltage across the cell under different externally applied voltages (biases), and the ammeter measured the current output from the cell. To calibrate the cell with the light source for testing, a few variables were adjusted. With known short-circuit current and open-circuit voltage specifications under one-sun conditions from the manufacturer, the power source was used to keep the solar cell at short-circuit conditions by outputting enough voltage to make the voltage difference zero across the cell terminals. Instead of physically connecting a wire between the front and rear contacts of the cell to short-circuit it and force the voltage difference to zero, this method uses the variable power source to drive the voltage difference to zero. The irradiance of the light source is then adjusted, keeping short-circuit conditions, until the current output matches

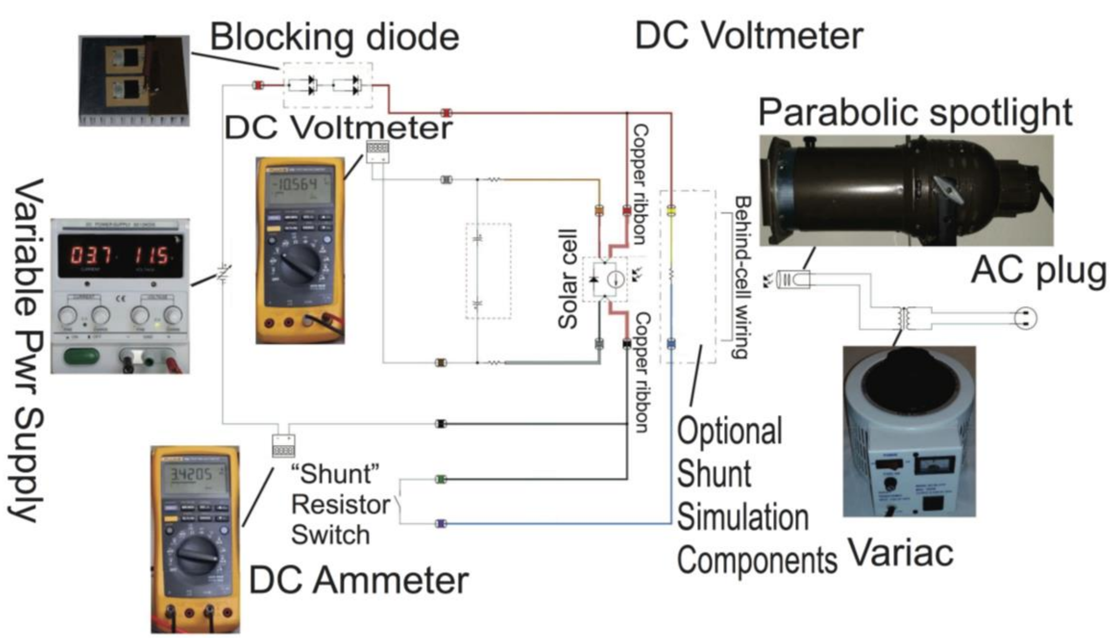

FIG. 2. Sample experimental setup (Figure from [19]). Shown are the various components used for testing. Note that the optional shunt simulation components and "shunt" resistor switch are not connected to the circuit for these tests.

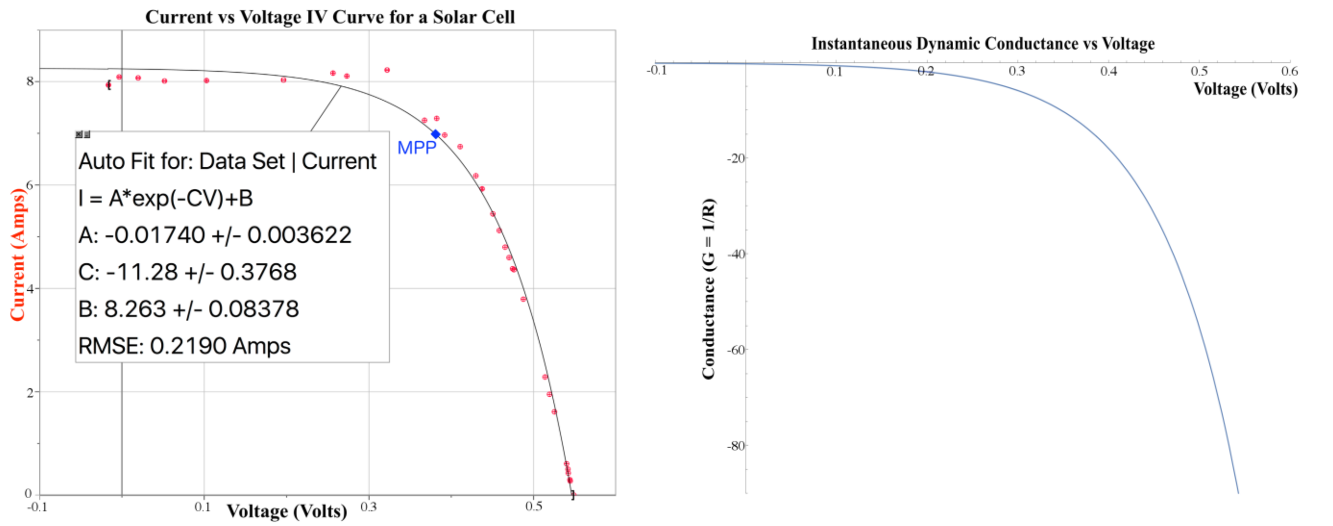

(a) (b)

FIG. 3. (a) IV curve for solar cell with maximum power point (MPP) marked, (b) instantaneous dynamic conductance of solar cell. Note that (b) shows the derivative of equation given by fitting the Shockley model to data in part (a).

the manufacturer specifications at one-sun. This method calibrates the light source to the cell. Heating by the spectrum of the light source is not important at this step, since the short-circuit current of the cell has a low temperature coefficient. In this short-circuit condition, the cell produces no power, resulting in the entire energy of the spectrum absorbed by the cell being converted to heat.

The IV curve sweep started with the cell in open-circuit conditions. The power source was then used to move the voltage experienced across the cell from open-circuit down to short-circuit, with a difference of zero volts across the terminals. Throughout the IV curve, data points were taken using voltage as the independent variable, and current as the dependent variable.

To confirm that dynamic conductance around the maximum power point is significantly higher than around short circuit, more data points were taken approximately 50-mV apart at both spots on the IV curve. By dividing the differences in current by differences in voltage in each section the dynamic conductances were found experimentally instead of relying on the derivative of the IV curve. While it is obvious that the dynamic conductance is the derivative at a single point of the IV curve, taking manual data was useful for additional confirmation.

After confirming that dynamic conductance drops toward zero as the cell approached reverse bias, another test was performed to show that under reverse bias conditions the cell does indeed start to heat up significantly. To examine this power dissipation, the supplied voltage was increased past short circuit to reverse bias, and the conditions of the cell were observed while the cell dissipated power. For this test, the cell was operated at 80% irradiance to emulate 20% shading across the cell. This condition was achieved by reducing the light level until 80% of the short-circuit current as specified by the manufacturer was measured with the cell held at zero volts.

IV. DATA ANALYSIS

A. Calculation of Dynamic Conductance

Fitting the voltage and current data points with the Shockley model produces a typical IV curve, as seen in Fig. 3(a). The magnitude of the dynamic conductance in this particular cell seems to drop off very quickly as voltage decreases, for the data points taken as the voltage approaches zero have a long stretch of nearly zero current change. There is also a small anomaly in the current measurements around 0.3V; the data points seem to momentarily jump up to higher current than in short-circuit conditions. Note, however, that a small change in applied voltage around maximum power point results in a relatively large change in current, but around short-circuit conditions even a large change in voltage has essentially no effect on the current output. Figure 3(b) demonstrates that the dynamic conductance, or the derivative of the IV curve, approaches zero as the voltage drops toward zero from a positive bias.

B. Hot Spots in Isolated Cells and in Cells in a String

Isolated Cell: While taking measurements for the IV curve and forcing the cell into reverse bias, thermal pictures were taken using the IR camera. Figure 4(left) shows the amount of heating present in short circuit, when no power is being converted to electricity. This figure is useful as a baseline to compare the temperature changes at maximum power point and in reverse bias. Figure 4(middle) in forward bias contrasts sharply with Fig. 4(right) in reverse bias. Note that every image in Fig. 4 uses the same color scaling. In Fig. 4(middle), the cell is

FIG. 4. Thermal images of a solar cell under different conditions: (left) the cell at short circuit (167.1°F or 75.1°C), (middle) the cell near maximum power generation (145.5°F or 63.1°C), (right) the cell under reverse bias (398.5°F or 203.6°C)

converting the maximum amount of light energy coming from the spotlight into electrical energy instead of heat, meaning that some of the energy that was being converted to heat is now leaving the system, effectively cooling the cell. In Figure 4(right) the cell is in reverse bias and is dissipating energy supplied by the power source instead of producing energy on its own.

Cells in a String: In a real-world situation the reverse bias would be produced by a partially-shaded cell driven to catch up to the current output of the fully-illuminated cells in its string. If the cell tries to develop a reverse bias greater than the accumulated voltage of the other cells in the string, the bypass diode activates and stops the reverse bias from becoming more extreme. However, in this manner bypass diodes only prevent reverse bias from increasing past a certain point, instead of preventing any reverse bias at all [12].

A cell in reverse bias still outputs a positive current, but now there is a voltage decrease in the direction of current flow instead of a voltage increase. Since $P=IV$, and the voltage has become negative, the power generation of the cell turns to power dissipation. It is this power dissipation that heats up the cell and causes hot spots. If the cell has defects caused by manufacturing error or weathering, these flaws have the possibility of providing easier pathways for current to flow, concentrating the power dissipation into small areas, instead of across the entire face of the cell. If the power dissipation is concentrated in a sufficiently small area, the heating could be significant enough to melt the solder, heat-cycle the cell, or in extreme cases melt the silicon in the cell.

The voltage difference across the cell in Fig. 4(right) is driven to –12 volts to simulate the accumulated voltage of a string of cells. A typical setup includes bypass diodes in parallel with a string of approximately 20 cells. If each of the other cells is fully illuminated, and they output a reasonable 0.6V each, then reverse bias around 12 volts can easily accrue. The 12 volts used reproduces the voltage from the 19 cells in forward bias along with the voltage drop across the bypass diode (typically another 0.6V or so).

It is useful to point out that these temperatures highlight the low melting point of solders often used in solar cells. Two typical solders are Sn96Ag4 with a melting point of 221°C (430°F), and Bi58Sn42, with a melting point of 138°C (280°F) [17, 18]. Note that the surface temperature of the solar cell under simulated reverse bias conditions exceeded the melting point of the Bi58Sn42 solder. While the cell was experiencing those conditions in the lab, the solder for the tabbing of the cells melted and the leads almost completely disconnected from the cell.

In a complete panel the leads do not often physically separate from the cell because the cell is encased in some other material such as glass, which usually keeps the leads and the cell in physical contact even if the solder melts. However, with heat cycling, the granularization of solder starts to become an issue as the crystals inside the solder become larger and larger as the different metals of the alloy separate out [17]. Given enough heat cycling it is theoretically possible for the grain size to cause localized disconnects between the cell and the leads, possibly causing plasma arcs [6].

This extreme heating can cause increased aging effects. It is interesting to note that one study of space-based solar cells found hot spots with temperatures up to 500°C. [3]

C. Results

Judging by the heating effects on the cell under externally applied reverse bias, it should be clear that such conditions should be avoided at all costs, lest the cell or surrounding panel suffer irreparable damage or lifetime degradation. Under normal operating conditions (forward bias), the cell cannot heat up enough to desolder the cell unless a similar surface outside would regularly reach temperatures of greater than 125°C (257°F).

Note that this temperature is hotter than the boiling point of water at standard atmospheric pressure. There are no places on earth where it would be feasible to place solar cells where they would reach temperatures that would cause danger to the components of the cell while in forward bias.

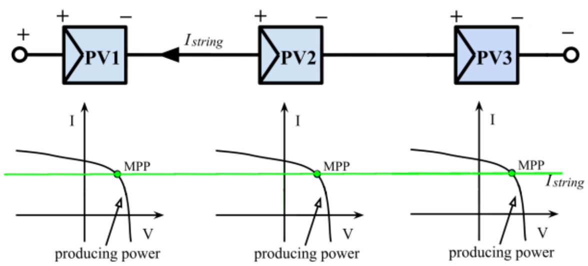

FIG. 5. Series solar cell diagram (Figure from [7]).

These temperatures however, can be reached when the cell dissipates power, and this heating problem only becomes more localized and exacerbated with defects in cell material.

D. Reverse Bias Prevention in PV Strings

Hot spots are surprisingly easy to prevent as long as the IV operating point on partially- or completely-shaded cells is adjusted to prevent reverse bias. A controller for a string that changes the total string voltage or current draw, so that all cells draw less current when one cell becomes partially shaded, should protect every cell from entering reverse bias and generating hot spots (see Figs. 5-7). This process would involve increasing the total string voltage and bringing the current down on the IV curve, and in doing so sacrifice some overall power output as the current decreases.

In Figs. 5-7, it is easy to see that without shading, the cell is operating perfectly fine at maximum power point in Fig. 5, but when partial shading occurs on one cell, the total current output drops, as seen in Fig. 6. In this situation a typical charge controller would still be seeking maximum power point for the string as a whole, and decreases voltage across the string enough to force the partially-shaded cell into reverse bias. The controller proposed by idealPV would track maximum power point while taking into account reverse bias, and tracks to the highest power output with no reverse bias or heating possible (Fig. 7).

E. Future Improvements

However, there are a great many possible areas for improvement or sources of error in this experiment. For one, the solar cells tested in the lab were always isolated, with reverse bias conditions applied using a power source. A more convincing argument would be made by observing these conditions in a typical commercial panel by physically partially shading one cell, looking at a system-level interaction among each cell in the panel and substrings and how reverse bias develops. For example, UL does testing of panels as a whole, and their method does not directly measure the voltage, current, and temperature of each cell in the panel at the same time [20].

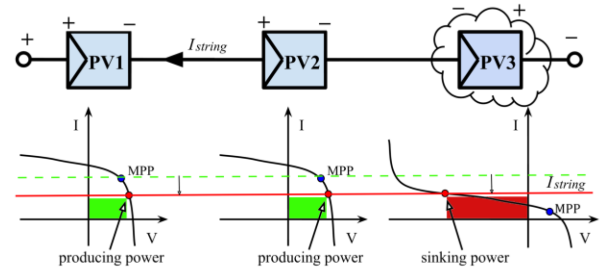

FIG. 6. Current mismatch and resulting reverse bias due to high current draw (Figure from [7]).

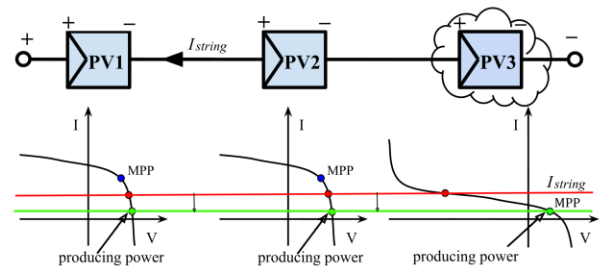

FIG. 7. The smart charge controller moves all operating points to forward bias (Figure from [7])

Additionally, the open-circuit voltage and short-circuit current of the solar cells were only superficially verified by the manufacturer, and were not guaranteed by an accompanying data sheet. The exact amount of light supplied by the spotlight may be slightly off, but a small change in irradiance does not have a significant effect on the method or results.

While these experiments were done in a temperature-controlled lab, the heat generated from the spotlight may introduce small errors or fluctuations in temperature measurements or might influence temperature calibration.

Also, the power source introduced occasional drift in voltage outputs that may create a small systematic bias in the IV curve calculations.

V. FIELD STUDY

This section includes the results from the field study and will be updated as we add in data and sections to the Final Report.

A. Setup and Purpose

This section will explain the purpose of the demonstration: how the two setups are different and the reason why the panels are in different directions with the introduced shade. See Figure 8.

FIG. 8. Photograph of the trailers at the field test site.

B. Daily Energy Collection

This section explains the energy collected each day from the panels, the main deliverable from the clinic study. It will explain the loss in data for the few days for the idealPV panels, and note the higher production of the idealPV setup over the conventional setup under these specific testing conditions. See Fig. 9.

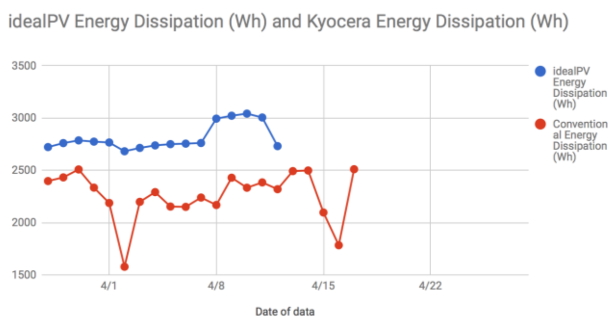

FIG. 9. Graph showing the daily energy output, in Wh, of idealPV (blue) and Kyocera (red) arrays over the course of the 26-day field study.

C. Thermal Data

Hopefully we will have some very high contrast hot spots by the time the field study is over to put here, but at the very least we can show that the idealPV panels do not have much temperature difference across the cells, while there is some difference in the conventional panels. The current difference of 49.0°C (120.2°F) to 31.8°C (89.2°F) between difference cells on the Kyocera panel is noticeable, but hopefully we can find greater contrasts for added effect. See Figures 10 and 11.

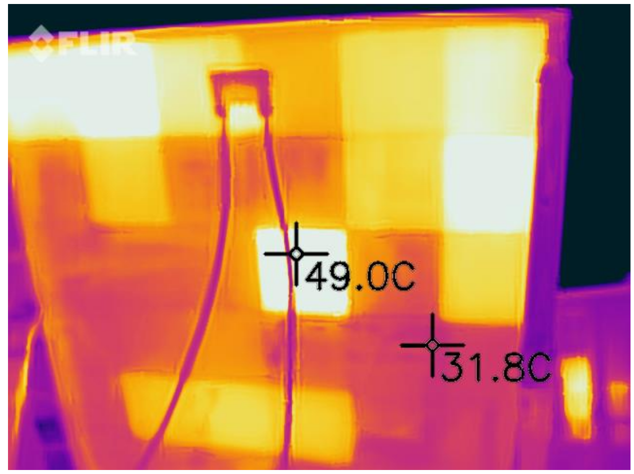

FIG. 10. Thermal image of the south-facing Kyocera panel on March 27, 2018 at 11am.

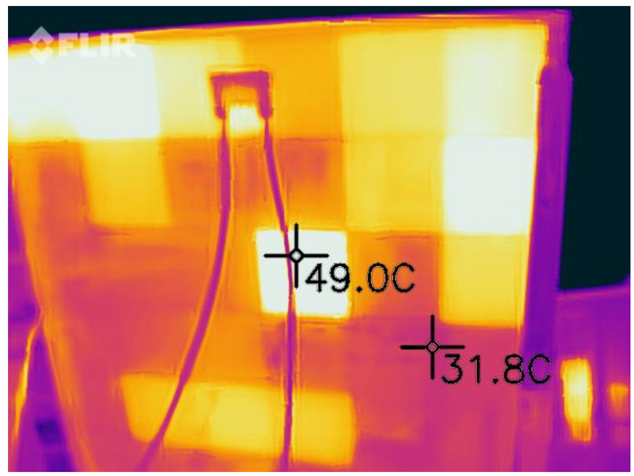

FIG. 11. Placeholder image for a good thermal image of an idealPV panel as contrast to conventional.

VI. CONCLUSION

Hot spot heating is a significant problem in the solar industry, and this heating is easily explained by cells entering reverse bias and dissipating power produced by other cells in the string. Therefore, it is useful to have a tool to predict when cells will enter into reverse bias in order to stop those conditions from happening. There are already measures for protecting against extreme cases of reverse bias in modern solar panels, such as bypass diodes, but none of the existing options actively monitor the dynamic conductance of the cells and predict reverse bias. Accurate, real-time monitoring of dynamic conductance can alert controllers to increase the total voltage on a string or decrease current draw until a current is reached that allows all cells to operate in forward bias. All cells will then be generating some power, while bypass diodes, for example, would bring the total power of the string to zero. Having no current mismatches due to shading prevents cells from dissipating power and heating up to damaging levels.

ACKNOWLEDGMENTS

This work was supported by the engineering and physics departments of Harvey Mudd and Pomona Colleges, with special acknowledgements to the other members of the HMC clinic team: Jonathan Kupfer, Florence Walsh, Dallon Asnes, and Quentin Barth. Many thanks also to faculty advisors Dick Haskell, Peter Saeta, Qimin Yang, and Tom Donnelly.

REFERENCES

[1] idealPV, "idealpv.com." http://idealpv.com, 2015.

[2] K. Kernahan and P. Curzon, "Empirical Evidence for Thermodynamics, Forward Only Zero Hot Spot and Reverse Bias Heating in Solar Cells." http://idealpv.com/idealPV_FOZHS_Empirical_Evidence_white_paper.pdf, 2015.

[3] J. C. Larue and E. du Trieu, *Effect of Partial Shadowing on Solar Panels Hot Spot or Breakdown?*, pp. 490–495. Dordrecht: Springer Netherlands, 1981.

[4] Dupont, "Mitigating strategies for hot spots in crystalline silicon solar panels." http://www.dupont.com/content/dam/dupont/products-and-services/solar-photovoltaic-materials/solar-photovoltaic-materials-landing/documents/hot-spot-mitigation.pdf.

[5] C.Honsberg and S. Bowden, "PVEDUCATION." http://www.pveducation.org/.

[6] L. Zhu, L. Fu, M. Qiao, B. Cui, Q. Chen, and J. Lin, "The characteristics of primary and secondary arcs on a solar array in low earth orbit," *PlasmaScience and Technology*, vol. 19, no. 5, 2017.

[7] K. A. Kim, G. S. Seo, B. H. Cho, and P. T. Krein, "Photovoltaic

Hot-Spot Detection for Solar Panel Substrings Using AC Parameter

Characterization," *IEEE Transactions on Power Electronics*,

vol. 31, pp. 1121–1130, Feb. 2016.

[8] T. Ghanbari, "Hot spot detection and prevention using a simple

method in photovoltaic panels," *IET Generation, Transmission*

Distribution, vol. 11, no. 4, pp. 883–890, 2017.

[9] J. Gallon, G. Horner, J. Hudson, L. Vasilyev, and K. Lu, "PV

Module Hotspot Detection," *NREL*, Feb. 2015.

[10] S. Guo, T. M. Walsh, A. G. Aberle, and M. Peters, "Analysing

partial shading of PV modules by circuit modelling," in *2012*

38th IEEE Photovoltaic Specialists Conference, pp. 002957–

002960, June 2012.

[11] K. A. Kim, C. Xu, L. Jin, and P. T. Krein, "A Dynamic

Photovoltaic Model Incorporating Capacitive and Reverse-

Bias Characteristics," *IEEE Journal of Photovoltaics*, vol. 3,

pp. 1334–1341, Oct. 2013.

[12] K. A. Kim and P. T. Krein, "Reexamination of Photovoltaic Hot

Spotting to ShowInadequacy of the Bypass Diode," *IEEE Journal*

of Photovoltaics, vol. 5, pp. 1435–1441, Sep. 2015.

[13] K. Kernahan, "Idealized solar panel." https://www.google.

com/patents/US8952672, Feb. 10 2015. US Patent 8,952,672.

[14] S. A. Spanoche, J. D. Stewart, S. L. Hawley, and I. E. Opris,

"Model-based method for partially shaded pv modules hot

spot suppression," in *2012 IEEE 38th Photovoltaic Specialists*

Conference (PVSC) PART 2, pp. 1–7, June 2012.

[15] A. M. I. Aldaoudeyeh, "Photovoltaic-battery scheme to enhance

pv array characteristics in partial shading conditions,"

IET Renewable Power Generation, vol. 10, no. 1, pp. 108–115,

2016.

[16] J. Nelson, *The Physics of Solar Cells*. Imperial College Press,

2003.

[17] T. Geipel, M. Moeller, A. Kraft, and U. Eitner, "A comprehensive

study of intermetallic compounds in solar cell interconnections and their growth kinetics," *Energy Procedia*,

vol. 98, no. Supplement C, pp. 86 – 97, 2016. Proceedings of

the Sixth Workshop on Metallization and Interconnection for

Crystalline Silicon Solar Cells.

[18] Techni-Tool, "Minimizing micro-cracks in solar cell

interconnection." http://www.techni-tool.com/

site/ARTICLE_LIBRARY/OK%20International%20-%

20Minimizing%20Micro-cracks%20in%20Solar%20Cell%

20Interconnection.pdf.

[19] idealPV, "Reverse Bias Experimental Station." https:

//www.hmc.edu/hcsed/energize-colleges-program/

internships/claremont-locally-grown-power-clgp/.

[20] Underwriters' Laboratories, *Standard for Flat-Plate PhotovoltaicModules*

and Panels, vol. 1703. third ed., 2015.